*Journal of Sound and Vibration* (1998) **213**(3), 551–560

# VIBRATION TRANSMISSION FROM DECK TO HULL VIA A BULKHEAD

R. C. N. Leung

*Defense Evaluation and Research Agency, Haslar, Gosport PO12 2AG, U.K.*

(*Received* 16 *October* 1996, *and in final form* 30 *January* 1998)

Machines on board a ship are mounted on decks, which are supported by bulkheads from the hull. This paper studies the vibration transmission characteristics along the transmission path of deck–bulkhead–hull. The model used in this study consists of two infinite parallel plates, representing a deck and a hull, connected by a single bulkhead. The excitation force is applied on the top plate, in the plane of the bulkhead. Thus, only in-plane waves exist in the bulkhead. The two infinite plates are assumed to have pure bending waves only. The analyses show that at low frequencies the two parallel plates are strongly coupled. At frequencies above the first resonance of the bulkhead due to shear waves, the two plates become uncoupled. The top plate, which the excitation is acted upon, exhibits the behaviour of a single infinite plate. The bottom plate, however, can be treated as a series of independent beam elements running perpendicular to the bulkhead.

## 1. INTRODUCTION

Machines on board a ship are mounted on decks which are supported by bulkheads. The bulkheads will either be the supports between decks, or between deck and hull. Inevitably, the bulkheads will be one of the transmission paths for the vibrations originated from the machines. References [1–3] studied the longitudinal and flexural vibration transmission through a right-angled joint formed by two plates. This paper studies the characteristics of a bulkhead in the vibration transmission from a deck to a hull. The present study only considers a point excitation on the deck, directly above a bulkhead as shown in Figure 1. This is equivalent to a case where the bulkhead is directly underneath a support of a machine. The seating for the machine will therefore have a high impedance for vibration isolation purpose. The case of a moment excitation was a separate study and its findings will be presented in the future.

Kurtze and Watters [4] studied the impedance of sandwich plates with periodic wall structure. However, their analysis assumed that the structures linking the two outer skins are rigid because the gap between the skins was small. Such assumption will not be valid when bulkheads between decks and hulls are concerned. The model used in this study consists of two parallel infinite plates connected by a single bulkhead. The excitation force was restricted to the plane of the bulkhead. Therefore, only in-plane wave motions exist in the bulkhead. The two parallel plates are assumed to have pure bending waves. The bottom plate is treated as an orthotropic plate to take into account that it is strengthened by stiffeners. This is normally the case for the hull of a ship.

The whole model was divided into three subsystems, two individual infinite plates and an infinite strip. The mobility method was used in coupling the three subsystems together. Since line contacts rather than point contacts are involved in the model, the coupling is performed in the wavenumber domain along the length of the connections. The model was

0022–460X/98/230551 + 10 $25.00/0/sv981530

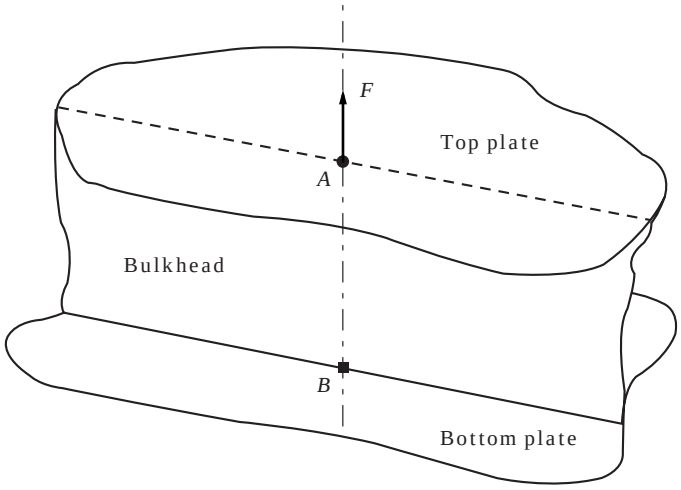


Figure 1. Model of Deck–Bulkhead–Hull.

further simplified by treating the top and bottom plates as two series of independent beam elements running perpendicular to the connections, and the bulkhead treated as a beam with shear waves only. These two simplifications give similar results for low frequencies, when the two plates are strongly coupled together.

## 2. MODEL OF SHIP STRUCTURE

The model used in this study consists of two infinite plates connected by a single bulkhead as shown in Figure 1. The top plate is assumed to be homogeneous of thickness $h_1$, a mass per unit area $m_1$, and a bending rigidity $D_1$. Whereas, the bottom plate is assumed to be orthotropic with an equivalent thickness $h_2$, a geometrically averaged mass per unit area $m_2$, and the bending rigidities in the $x$ and $z$ directions as $D_x$ and $D_z$ respectively. The bulkhead is homogeneous with a thickness $b$, a height $\ell$, and a mass per unit area $m_b$. The bulkhead lies in the $x$–$y$ plane. A normal excitation force is applied at the top plate at point A, which is in the plane of the bulkhead. The point A falls in line with the origin of the $x$–$z$ plane. Point B is a point on the bottom plate directly under Point A. This study concentrates on the responses at points A and B with respect to a normal force at point A.

Although, in general, decks are supported by a number of bulkheads. If the bulkheads are assumed to be widely spaced and the plates are heavily damped, no standing waves will be established on the plates between bulkheads. Therefore, from the viewpoints at A and B, the top and bottom plates can then be treated as two infinite plates.

## 3. POINT AND TRANSFER ACCELERANCE IN VACUUM

The analysis of the model was carried out by dividing the model into three subsystems—top plate, bulkhead and the bottom plate, and then coupling them together using the mobility method. It is necessary to express the responses of the subsystems in the wavenumber, $k_x$, domain because the subsystems are coupled together along a line. The Fourier transform pair for the space, $x$, and wavenumber, $k_x$, is defined as:

$$g(k_x) = \int_{-\infty}^{\infty} e^{ik_x x} f(x)\, dx; \qquad f(x) = \frac{1}{2\pi} \int_{-\infty}^{\infty} e^{-ik_x x} g(k_x)\, dk_x$$

and the Fourier transform pair for the time, $t$, and frequency, $\omega$, is defined as:

$$g(\omega) = \int_{-\infty}^{\infty} e^{-i\omega t} f(t)\, dt; \qquad f(t) = \frac{1}{2\pi} \int_{-\infty}^{\infty} e^{i\omega t} g(\omega)\, d\omega.$$

These definitions correspond to the convention of $e^{i(\omega t - k_x x)}$.

Consider the uncoupled model with an external applied stress distribution, $\sigma_e(k_x, \omega)$, on the top plate as shown in Figure 2. The displacement at the top plate, $w_1(k_x, \omega)$, along the $x$-axis at location 1 along the $x$-axis is governed by equation (1)

$$\ddot{w}_1(k_x, \omega) = \frac{-k_B^2}{4m_1}\left[\frac{1}{(k_x^2 - k_B^2)^{1/2}} - \frac{1}{(k_x^2 + k_B^2)^{1/2}}\right](\sigma_e(k_x, \omega) - \sigma_1(k_x, \omega))$$

$$= -\omega^2 I_1(k_x, \omega)(\sigma_e(k_x, \omega) - \sigma_1(k_x, \omega)). \tag{1}$$

The stresses in the bulkhead at location 2 and 3 are given by

$$\sigma_2(k_x, \omega) = bA_p(k_x, \omega)\ddot{w}_2(k_x, \omega) - bA_{tr}(k_x, \omega)\ddot{w}_3(k_x, \omega) \tag{2}$$

$$\sigma_3(k_x, \omega) = -bA_p(k_x, \omega)\ddot{w}_3(k_x, \omega) + bA_{tr}(k_x, \omega)\ddot{w}_2(k_x, \omega) \tag{3}$$

where $A_p(k_x, \omega)$ and $A_{tr}(k_x, \omega)$ are the direct and transfer apparent masses (stress/acceleration) of the bulkhead (Appendix A). Equations (2) and (3) assume that the thickness of the bulkhead, $b$, is small and that the displacement and stress will be uniform across the thickness.

The displacements of the bottom orthotropic plate, $w_4(k_x, \omega)$, at locations along the $x$-axis are governed by the equation:

$$\ddot{w}_4(k_x, \omega) = \frac{-k_{Bx}k_{Bz}}{4m_2}\left[\frac{1}{(k_x^2 - k_{Bx}^2)^{1/2}} - \frac{1}{(k_x^2 + k_{Bx}^2)^{1/2}}\right]\sigma_4(k_x, \omega)$$

$$= -\omega^2 I_4(k_x, \omega)\sigma_4(k_x, \omega). \tag{4}$$

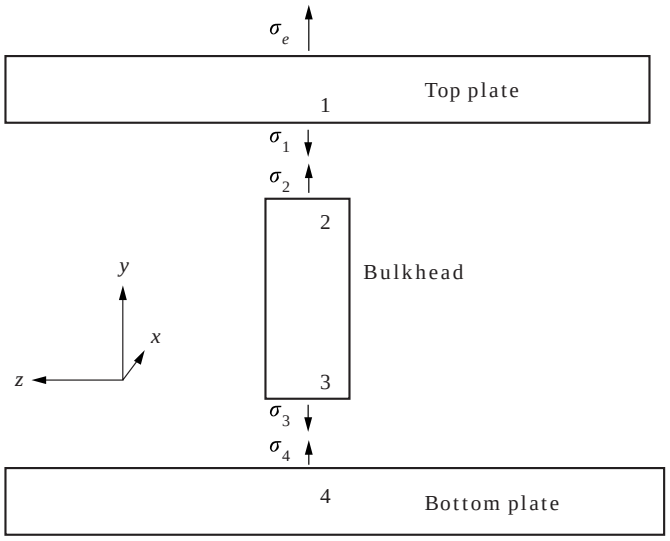


Figure 2. Block diagram of uncoupled system.

The boundary conditions for locations 1, 2, 3 and 4 once they are coupled together are:

$$\sigma_1(k_x, \omega) = \sigma_2(k_x, \omega); \qquad \sigma_3(k_x, \omega) = \sigma_4(k_x, \omega);$$
$$w_1(k_x, \omega) = w_2(k_x, \omega); \qquad w_3(k_x, \omega) = w_4(k_x, \omega). \tag{5}$$

Applying the boundary conditions to equations (1)–(4), the direct and transfer accelerances (acceleration/stress), $I_d(k_x, \omega)$, and $I_t(k_x, \omega)$ for the coupled system become:

$$I_d(k_x, \omega) = \ddot{w}_1(k_x, \omega)/\sigma_e(k_x, \omega) = [-bA_p(k_x, \omega)\omega^4 I_1(k_x, \omega)I_4(k_x, \omega) + \omega^2 I_1(k_x, \omega)]/X \tag{6}$$

and

$$I_{tr}(k_x, \omega) = \ddot{w}_4(k_x, \omega)/\sigma_e(k_x, \omega) = -bA_{tr}(k_x, \omega)\omega^4 I_1(k_x, \omega)I_4(k_x, \omega)/X \tag{7}$$

with the characteristic function $X$, given by

$$X = \omega^4 I_1(k_x, \omega)I_4(k_x, \omega)b^2[A_{tr}^2(k_x, \omega) - A_p^2(k_x, \omega)] + \omega^2[I_1(k_x, \omega) + I_4(k_x, \omega)]bA_p(k_x, \omega) - 1. \tag{8}$$

The stresses at the junctions are

$$\frac{\sigma_1(k_x, \omega)}{\sigma_e(k_x, \omega)} = 1 - \frac{bA_p(k_x, \omega)\omega^2 I_4(k_x, \omega) - 1}{X} \tag{9}$$

and

$$\frac{\sigma_4(k_x, \omega)}{\sigma_e(k_x, \omega)} = \frac{\omega^2 I_1(k_x, \omega)bA_{tr}(k_x, \omega)}{X}. \tag{10}$$

In the case where a point force, $F(\omega)$, is applied at the top plate, in the plane of the bulkhead, the applied stress is $\sigma_e(x, z, \omega) = F(\omega)\delta(x)\delta(z)$, with the origin of the coordinates coincides with the point force. The thickness of the bulkhead is assumed to be small compared with its height. Therefore, the responses $\ddot{w}_1(x = 0, \omega)$ and $\ddot{w}_4(x = 0, \omega)$ are the inverse Fourier transform of equations (6) and (7) at $x = 0$.

$$\ddot{w}_1(x = 0, \omega) = \frac{F(\omega)}{2\pi} \int_{-\infty}^{\infty} I_d(k_x, \omega)\, \mathrm{e}^{-ik_x x}\, \mathrm{d}k_x|_{x=0}$$

or

$$I_p = \ddot{w}_1(x = 0, \omega)/F(\omega) = \frac{1}{2\pi} \int_{-\infty}^{\infty} I_d(k_x, \omega)\, \mathrm{d}k_x \tag{11}$$

and

$$\ddot{w}_4(x = 0, \omega) = \frac{F(\omega)}{2\pi} \int_{-\infty}^{\infty} I_{tr}(k_x, \omega)\, \mathrm{e}^{-ik_x x}\, \mathrm{d}k_x|_{x=0}$$

or

$$I_{tr}(\omega) = \ddot{w}_4(x = 0, \omega)/F(\omega) = \frac{1}{2\pi} \int_{-\infty}^{\infty} I_{tr}(k_x, \omega)\, \mathrm{d}k_x \tag{12}$$

The point and transfer accelerance $I_p(\omega)$ and $I_{tr}(\omega)$ are given in integral form because closed form solutions for both equations are not possible. They are evaluated using

numerical methods. The results for a steel top plate of 10 mm thick, a bulkhead of 10 mm thick and 3 m high, and a bottom steel plate of 50 mm thick with the bending rigidity in the $z$-direction strengthened to an equivalent thickness of 360 mm, are shown in Figure 3. The responses of an infinite plate of 10 mm thick and of an infinite plate with its neutral axis offset by 1·5 m are also plotted on the same graph for comparison. The figure shows that at low frequencies, the two plates are strongly coupled together. They move together as a single body. As the frequency increases, the two plates start to decouple from each other. The top plate approaches the behaviour of an infinite plate at frequencies well above 10 kHz.

## 4. SHEAR BEAM APPROXIMATION

The model in Figure 1 was further simplified by making the following assumptions:

(a) The top and bottom plates are soft in flexure compared with the bulkhead. They are then treated as a series of independent beam elements of width d$x$, running perpendicular to the length of the bulkhead. The beam elements have the flexural rigidity of a plate of the same thickness.
(b) The bulkhead is treated as a beam with plane shear waves. There is no wave motion along the height of the bulkhead, i.e. the responses of the top and the bottom plates are the same.

Consider a single beam element of width d$x$, as shown in Figure 4. The equation of motion for the element d$x$ is

$$\frac{\partial^2 \dot{w}(x,\omega)}{\partial x^2} + \frac{\omega^2 m_b}{Gb}\,\dot{w}(x,\omega) - \frac{i\omega}{G\ell b}\,(Z_1(\omega) + Z_2(\omega))\dot{w}(x,\omega) = \frac{-i\omega}{G\ell}\,\sigma(x,\omega) \qquad (13)$$

where $Z_1(\omega)$ and $Z_2(\omega)$ are the impedance of the infinite beams for the top and bottom beam elements respectively.

$$Z_1(\omega) = \frac{2\omega m_1}{k_B}\,(1+i); \qquad k_B^4 = \frac{\omega^2 m_1}{D};$$

and

$$Z_2(\omega) = \frac{2\omega m_2}{k_{Bz}}\,(1+i); \qquad k_{Bz}^4 = \frac{\omega^2 m_2}{D_z}.$$

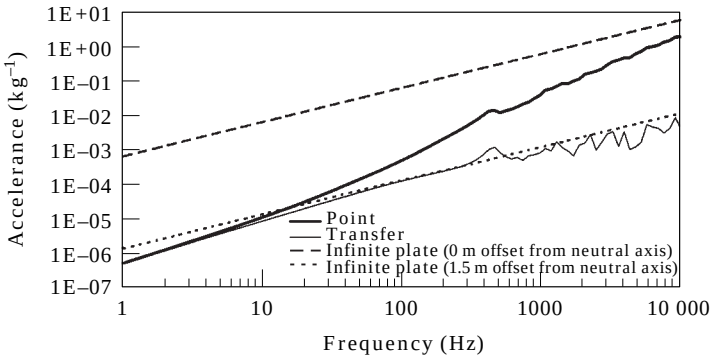


Figure 3. Point and transfer accelerances.

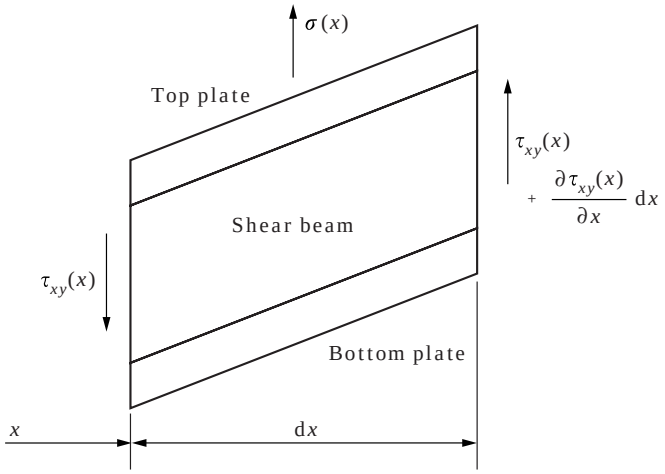


Figure 4. A shear beam element of width d$x$.

For a force over the width of the shear beam, $\sigma(x) = (F/b)\delta(x)$, the response at the excitation point is given as

$$\ddot{w}(x=0) = \frac{-i\omega^2 F}{2G\ell b\left[k_s^2 - \dfrac{i\omega}{G\ell b}\left(Z_1(\omega) + Z_2(\omega)\right)\right]^{1/2}} \tag{14}$$

where $k_s$ is the shear wavenumber of the shear beam. The square-root term in equation (14) is taken such that the imaginary part is positive. Figure 5 compares the shear beam approximation with the point and transfer accelerance derived in the previous section.

## 5. EXPERIMENT

An experimental rig was erected to simulate the Deck–Bulkhead–Hull model. It was made up of two 1·8 m × 1·8 m × 5 mm perspex sheets, and a perspex strip of size 1·8 m × 305 mm × 5 mm. The strip was glued to the two sheets forming an I-section structure. The whole rig was then rested on its end on a layer of foam. An electro-magnetic

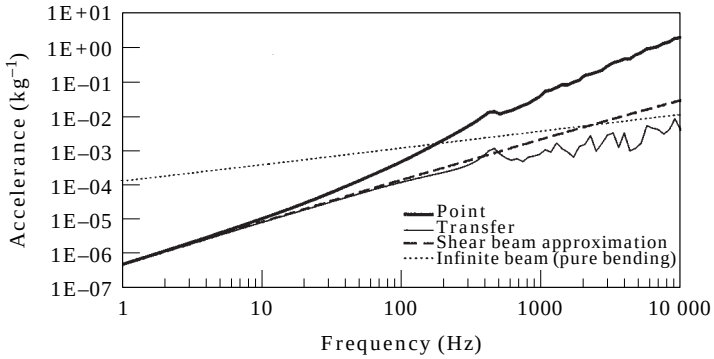


Figure 5. Shear beam approximation.

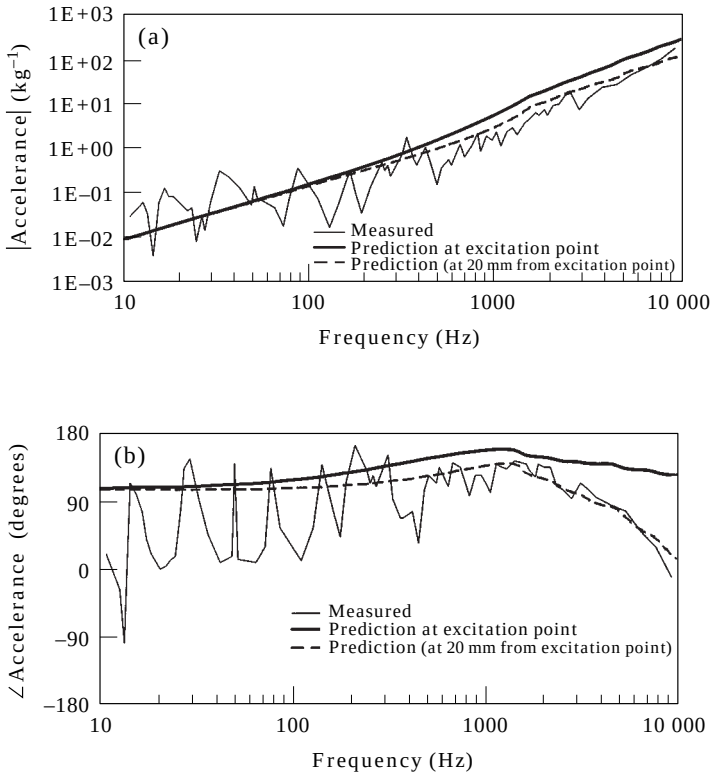


Figure 6. Measured point accelerance.

shaker with a force transducer was placed at the centre of one of the two perspex sheets. Two accelerometers were attached to the rig. One was placed adjacent to the force transducer. Another was placed at the centre of the other perspex sheet directly in line with the shaker. The force and the accelerations were measured simultaneously when a rapid swept sine excitation signal was fed to the shaker. The point and transfer accelerances, were calculated by taking the average of a number of excitations. Figures 6 and 7 show the measured point and transfer accelerances (accelerations/force). The measurements exhibit resonant behaviour even at frequencies below 100 Hz. This is because the experimental rig was made of finite perspex sheets. The resonances at low frequencies were the flexural resonances of the perspex sheets, with wave motions perpendicular to the bulkhead. The bulkhead moves more or less in phase along its length. At high frequencies, the resonances were a combination of flexural resonances of the perspex sheets and the resonances of the shear and dilatational waves of the perspex strip. Figure 6(a) shows that the modulus of the measured point accelerance has a similar trend to that of the theory. At frequencies below 400 Hz, the theoretical prediction represented the mean line of the measured results. At higher frequencies, the measured accelerance was lower than the theoretical values. This discrepancy was due to the fact that the measured result was not exactly the point accelerance since the accelerometer was placed adjacent to a force transducer, the distance between the axes of the accelerometer and force transducer was about 20 mm. The magnitude and phase predictions of the response at a point 20 mm from the excitation point were calculated and plotted in Figures 6(a) and 6(b). They showed good agreements with the measurements over the whole frequency range.

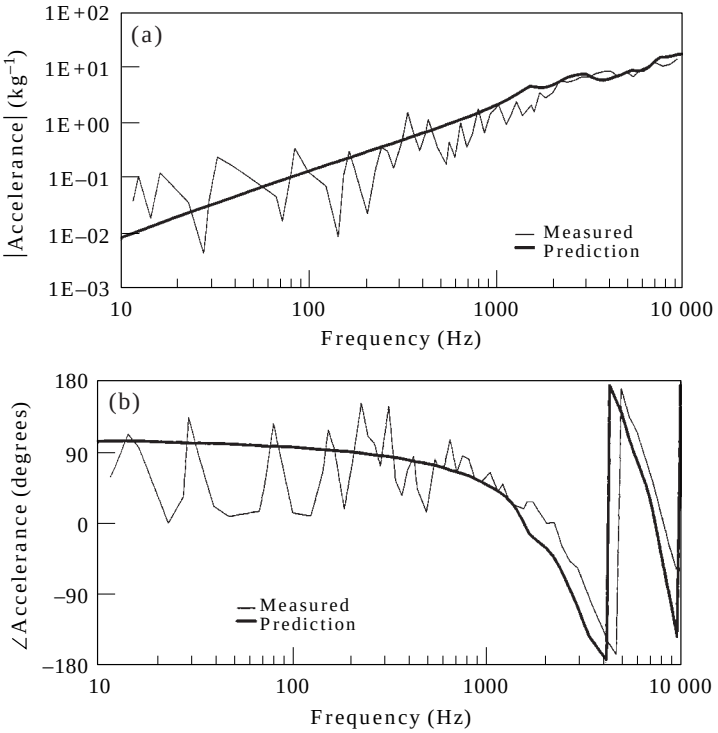


Figure 7. Measured transfer accelerance.

Figure 7 shows the transfer accelerance between the acceleration at the centre of the other perspex sheet directly in line with the excitation point. The measured accelerance agreed with the theoretical prediction, taking into account the finite nature of the rig.

## 6. DISCUSSION

A model of two infinite plates connected by a single infinite strip was used to represent the deck of a ship supported to the hull by a bulkhead. The point and transfer accelerances were derived. They showed that the top and bottom plates move anti-symmetrically with respect to the natural axis, along the junctures, at low frequencies. At high frequencies, the two plates decoupled. The behaviour of the top plate tends towards a single infinite plate. The response of the bottom plate at the intersection with the bulkhead becomes dominated by the shear wave motion of the bulkhead once decoupled. The first resonance due to the existence of a standing shear wave across the height of the bulkhead can be treated as the decoupling frequency.

At low frequencies, before decoupling, the whole model can be simplified further by treating it as a beam only with plane shear waves coupled with a series of independent flexural beam elements on the top and bottom of the beam.

The theoretical prediction agreed with experimental measurements obtained from a perspex model in the laboratory. The model was also found to be a good representation when compared with some actual measurements taken from a vessel in dry dock.

The derivation of the point and transfer accelerances presented in this paper allows the modelling of structures made up of subsystems with line connections.

## REFERENCES

1. L. Cremer and M. Heckl 1973 *Structure-borne Sound*. Berlin: Springer.
2. R. C. N. Leung and R. J. Pinnington 1990 *Journal of Sound and Vibration* **142**, 31–48. Wave propagation through right-angled joints with compliance-flexural incident wave.
3. R. C. N. Leung and R. J. Pinnington 1992 *Journal of Sound and Vibration* **153**, 223–237. Wave propagation through right-angled joints with compliance: longitudinal incident wave.
4. G. Kurtze and B. G. Watters 1959 *Journal of the Acoustical Society of America* **31**, 739–748. New wall design for high transmission loss or high damping.
5. A. E. H. Love 1944. *The Mathematical Theory of Elasticity*. New York: Dover.

## APPENDIX A BLOCK APPARENT MASS OF AN INFINITE STRIP

Consider a two dimensional element of size $\mathrm{d}x\ \mathrm{d}y$ with a mass per unit area $m$ as shown in Figure A1. The two independent wave equations are [5]

$$\nabla^2\varepsilon = \frac{1}{c_1^2}\frac{\partial^2\varepsilon}{\partial t^2} \tag{A1}$$

$$\nabla^2\psi = \frac{1}{c_2^2}\frac{\partial^2\psi}{\partial t^2} \tag{A2}$$

with $c_1^2 = (\lambda + 2\mu)/m$ and $c_2^2 = \mu/m$, the dilatational and rotational wave speeds. $\lambda$ and $\mu$ are the Lamé constants.

Fourier transforming (A1) and (A2) into the frequency domain gives

$$\nabla^2\varepsilon(\omega) + k_1^2\varepsilon(\omega) = 0 \tag{A3}$$

$$\nabla^2\psi(\omega) + k_2^2\psi(\omega) = 0 \tag{A4}$$

with $k_1 = \omega/c_1$ and $k_2 = \omega/c_2$, the dilatational and rotational wavenumbers respectively.

Fourier transforming (A3) and (A4) into the wavenumber domain, $k_x$, gives

$$\frac{\mathrm{d}^2}{\mathrm{d}y^2}\varepsilon(k_x, \omega) - (k_x^2 - k_1^2)\varepsilon(k_x, \omega) = 0 \tag{A5}$$

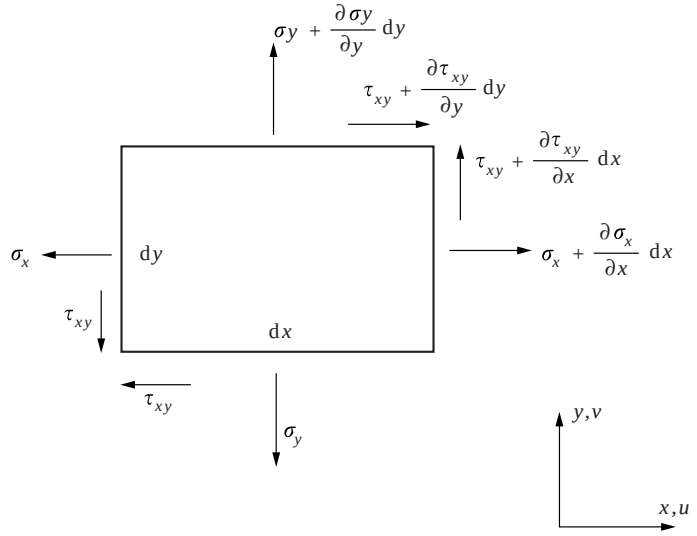


Figure A1. A two-dimensional element of size $\mathrm{d}x\ \mathrm{d}y$.

$$\frac{d^2}{dy^2}\psi(k_x, \omega) - (k_x^2 - k_2^2)\psi(k_x, \omega) = 0. \tag{A6}$$

The solutions for (A5) and (A6) are

$$\varepsilon(k_x, \omega) = A_1 e^{k_\varepsilon y} + B_1 e^{-k_\varepsilon y} \tag{A7}$$

$$\psi(k_x, \omega) = A_2 e^{k_\psi y} + B_2 e^{-k_\psi y} \tag{A8}$$

with $k_\varepsilon^2 = k_x^2 - k_1^2$ and $k_\psi^2 = k_x^2 - k_2^2$.

Consider the case when the boundary $y = 0$ is blocked and an excitation wave with wavenumber $k_x$ and displacement amplitude $V$ is applied on the boundary $y = \ell$, the boundary conditions will be

$$\text{(i) at } y = 0 \quad u(k_x, \omega) = 0; \qquad v(k_x,\omega) = 0 \tag{A9}$$

$$\text{(ii) at } y = \ell \quad u(k_x, \omega) = 0; \qquad v(k_x, \omega) = V. \tag{A10}$$

Applying the boundary conditions to (A7) and (A8), the constants $A_1$, $A_2$, $B_1$ and $B_2$ can then be determined. The stresses at both boundaries $y = 0$ and $y = \ell$ can be determined as

$$\sigma_y(k_x, \omega)|_{y=0} = \frac{m[k_\psi k_x^2 \sinh(k_\varepsilon \ell) - k_\psi^2 k_\varepsilon \sinh(k_\psi \ell)]}{D} \ddot{V}(k_x, \omega) \tag{A11}$$

$$\sigma_y(k_x, \omega)_{y=\ell} = \frac{m[k_\psi k_x^2 \cosh(k_\psi \ell) \sinh(k_\varepsilon \ell) - k_\varepsilon k_\psi^2 \sinh(k_\psi \ell) \cosh(k_\varepsilon \ell)]}{D} \ddot{V}(k_x, \omega) \tag{A12}$$

with

$$D = 2k_x^2 k_\varepsilon k_\psi [\cosh(k_\varepsilon \ell) \cosh(k_\psi \ell) - 1] - (k_\varepsilon^2 k_\psi^2 + k_x^4) \sinh(k_\varepsilon \ell) \sinh(k_\psi \ell).$$

## APPENDIX B: NOMENCLATURE

| | |
|---|---|
| $b$ | thickness |
| $c_1, c_2$ | dilatational and rotational wavespeeds |
| $h_1, h_2$ | thicknesses |
| $k_x$ | wavenumber in $x$ |
| $k_1, k_2$ | dilatational and rotational wavenumbers |
| $\ell$ | height |
| $m$ | mass per unit area |
| $t$ | time |
| $u, v, w$ | displacements |
| $A$ | apparent mass (i.e. force/acceleration) |
| $D$ | bending rigidity |
| $E$ | Young's modulus |
| $F$ | force |
| $G$ | shear modulus |
| $I$ | accelerance (i.e. acceleration/force) |
| $Z$ | impedance (i.e. force/velocity) |
| $\varepsilon$ | dilatation |
| $\lambda, \mu$ | Lamé constants |
| $\nu$ | Poisson ratio |
| $\sigma$ | normal stress |
| $\tau$ | shear stress |
| $\psi$ | rotation |
| $\omega$ | angular frequency. |